Progress In Electromagnetics Research, Vol. 124, 151–162, 2012

PROPOSAL OF CYLINDRICAL ROLLED-UP METAMATERIAL LENSES FOR MAGNETIC RESONANCE IMAGING APPLICATION AND PRELIMINARY EXPERIMENTAL DEMONSTRATION

Y. Xie[1, 2], J. Jiang[1], and S. He[1, 2, 3, *]

[1]Centre for Optical and Electromagnetic Research, JORCEP [KTH-LTU-ZJU Joint Research Center of Photonics], Zijingang Campus, Zhejiang University (ZJU), East Building #5, Hangzhou 310058, China

[2]ZJU-SCNU Joint Research Center of Photonics, South China Normal University, Guangzhou 510006, China

[3]Department of Electromagnetic Engineering, School of Electrical Engineering, Royal Institute of Technology (KTH), Stockholm S-10044, Sweden

Abstract—In this paper, we propose a cylindrical rolled-up negative permeability metamaterial (MM) lens for magnetic resonance imaging (MRI), and some analyses are given. The proposed cylindrical MM lens is fabricated by rolling a MM slab (constituted with capacitive-loaded copper split rings) into a tube that resembles a hollow ring. It can focus the field of a magnetic line source, which can increase the penetration depth and improve the sensitivity of a surface coil. The proposed cylindrical MM lens can also improve the discrimination of the signals coming from two independent sources. A clinical experiment is carried out in a General Electric Signa 1.5 T MRI system in order to verify the focusing ability of the proposed device.

1. INTRODUCTION

In 2000, Pendry proposed that a type of lens with effective permittivity and permeability values both equal to -1 can compensate for wave decay and reconstruct images with a resolution better than the diffraction limit, which is also known as the "superlensing effect" [1]. Furthermore, due to the resonant nature of metamaterials (MM) it

Received 14 December 2011, Accepted 10 January 2012, Scheduled 18 January 2012

* Corresponding author: Sailing He (sailing@kth.se).

was shown that the parameters of the material are extremely sensitive and highly dispersive (in particular, the index must equal to -1 for the implementation of a superlens). A small deviation may make the subwavelength resolution unobservable, which causes MM superlenses to have a limited usable frequency range [1]. Fortunately, the narrow-band response is not a problem for magnetic resonance imaging (MRI) applications since MR images are acquired by measuring radiofrequency (RF) signals inside a relatively narrow bandwidth (only several kHz [2]). The application of MM in clinical research, e.g., MRI has previously been explored in a few works [3–7]. In all these works, the chosen MM components are non-ferromagnetic so that they do not interact with the static magnetic field, while the RF magnetic field can interact with internal resonant elements of MM. It has been shown that a MM slab with exotic permeability $\mu_r = -1$ can dramatically increase the sensitivity of MRI [3], and such a MM lens has been constructed [4]. They found that the lens has the ability to probe significantly deeper and it could also improve the image quality.

In clinical experiments, MRI is used to distinguish pathologic tissue (such as brain [8] and breast tumors [9]) from normal tissue. One advantage of an MRI scanner is that it is harmless to the patient. However, there are still some problems in improving spatial resolution without increasing the static magnetic field strength if we want to image some tiny spot and deep area in, for example, the brain [10]. Here we propose a new way to make a MM lens that could be used to boost the spatial resolution of MRI. The technique involves designing a MM slab with capacitive-loaded copper loops and then rolling up the slab into a tube that resembles a hollow ring. Thanks to their superior properties, the rolled-up lens has the advantage of easy fabrication, subwavelength confinement, low loss, and flexibility. Our lens is employed to increase the penetration depth of a standard surface coil and collimate the RF flux coming from deep tissue. In the present work, a real MM lens is fabricated and analyzed for MRI application. Both discrimination of two independent sources and focusing of field distribution are analyzed numerically, and an experiment is carried out in order to check the ability of the proposed device to focus the field.

2. MODELING

As mentioned above, the rolled-up MM lens suggested for MRI applications employs an idea of imaging objects with a sufficiently subwavelength structure having negative permeability or permittivity in the near field [6]. Before going further with our design, we must note that the RF field used for MRI has an associated wavelength much

higher than the dimensions of any practical coil. Therefore, our study is in the region of quasi-magnetostatics, and a MM lens with $\mu_r = -1$ should be enough for manufacturing the lens [1]. Due to Lorentz reciprocity [11], the sensitivity of a coil is directly proportional to the intensity of the magnetic field created by the coil (with a standard value for the current) inside the body of the patient. Fig. 1 sketches the configurations under analysis. The lens is dispersive and formed by capacitive-loaded copper loops. The artificial MM lens is modeled by the continuous medium approach [12]. The homogeneous rolled-up MM lens is designed with R (10 cm) as the inner radius and D (3 cm) as thickness. The practical MM lens composed with SRR is etched on the FR4 substrate with permittivity $\bar{\varepsilon} = \varepsilon_r - i\delta = \varepsilon_r - i\sigma/\omega\varepsilon_0$, where σ is conductivity of material, ε_0 is the permittivity in vacuum and ω is the angular frequency. Here, for two-dimensional (2D) numerical simulations, we choose $\bar{\varepsilon} = 4.2 - j0.02$ experimentally. The homogenous magnetic permeability of this medium was computed from Eq. (13) in Ref. [12] (but with different geometrical parameters) in order to obtain an isotropic artificial medium with $\mu_r = -1$ at 63.855 MHz, i.e., the Larmor frequency of 1.5 T MRI system.

MRI coils are usually placed just on the skin of the patient and used to obtain images of tissues in the proximity of the coil. The coils are designed to have localized field patterns and their sensitivity is restricted to a finite region of space, i.e., the sensitivity of surface

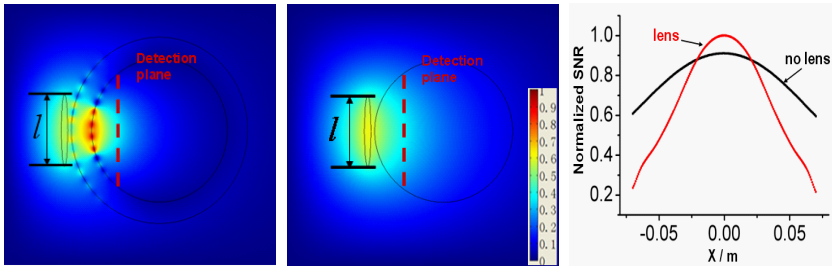

(a) (b) (c)

Figure 1. The field distribution when the finite size coil is placed on top of the rolled-up lens. The rolled-up lens has R (10 cm) for the inner radius and D (3 cm) for thickness with the effective permeability $\mu_r = -1$. The source with normalized current density is set to 10 cm long and 1 cm wide. The permittivity of normal tissue inside the MM lens is $\varepsilon \approx 21$, conductivity is $\sigma = 0.11$. (a), (b) Magnetic field patterns with and without the lens, respectively; (c) The cross-sectional plot of normalized SNR at the selected detection plane.

coils, as well as the signal to noise ratio (SNR), decreases rapidly with the distance from the coil [13]. In the numerical simulations, the tissue (e.g., breast, brain) is modeled as a cylindrical phantom inside the rolled-up MM lens. Joines et al. [18] have measured the electrical properties of normal and malignant human tissues for 50 to 900 MHz. We have obtained the effective dielectric constant from their work: take the breast as example, at the resonance frequency of 63.855 MHz, for normal breast tissue we have $\varepsilon \approx 21$ and $\sigma = 0.11$, while for the malignant breast tissue we have $\varepsilon \approx 80$ and $\sigma = 0.77$. Figs. 1(a), (b) show the focusing of magnetic field distribution with and without the MM lens, respectively. The homogenous lens is 10 cm in the inner radius and 3 cm thick. The source with normalized current density is set to 10 cm long and 1 cm wide. It is clearly demonstrated that a better focusing spot is formed with the help of the rolled-up lens. Meanwhile, due to Lorentz reciprocity [11], the sensitivity of a coil is directly proportional to the intensity of the magnetic field created by the coil. Furthermore, for comparison of the SNR we simply assume that SNR is proportional to the quantity $B/\sqrt{R}$ [3], where B is the magnetic field and R is the noise resistance defined in Ref. [3]. Fig. 1(c) shows that the MM lens can give a better SNR in the central focusing area. Anyway, there are significant noises in the vicinity of the inner surface of MM lens due to the additional noise introduced by the lens (see in Fig. 1(a)) and it has strong impact on SNR, which is demonstrated in Ref. [15].

However, further improvement of the focusing property is difficult due to the MM loss [14, 15]. The thickness of the lens (and thus the detection depth) is generally limited, and is restricted to near field detection. Meanwhile, for the safety of humans, the U.S. Food and Drug Administration and other healthcare safety groups have placed strict limits on the field strengths [2]. Since the rolled-up MM lens can help to focus the fields produced by individual coils at deeper distances inside the patient body, this device could be used to improve the sensitivity of the surface coil and lead to new perspectives on MRI target detection and imaging.

3. EXPERIMENTAL VALIDATIONS

For the experiments, the ideal MM lens was mimicked by a rolled-up slab consisting of a three-dimensional (3D) array of copper metallic rings loaded with non-magnetic capacitors [4]. Fig. 2(a) shows a sketch of the proposed device. The parameters are carefully chosen based on the analytical model in [16]. The fabricated split-rings have a diameter of 11.34 mm and a strip width of 2.02 mm, while the thickness

of copper is 0.3 mm. Each split-ring in the array contains a $470 \pm 1\%$ pF nonmagnetic capacitor for resonance at a specific frequency. The rings were etched on a FR4 substrate based on the printed circuit board technology. The rolled-up MM lens consists of 5 parts of $16 \times 3 \times 2$ cubic cells with a periodicity of 15 mm. These 5 parts of the device were connected with each other with belts to form a circular shape (see Fig. 2(a)), so the structure is flexible and can be open or folded. The magnetic permeability of this medium was computed from Eq. (13) in Ref. [12] in order to obtain an isotropic artificial medium with $\mu_r = -1$ as a function of the periodicity, the ring resistance, the ring self-inductance and the frequency of resonance. The resonant working frequency of our MM lens is designed to be 63.58 MHz, which corresponds to the Larmor frequency of the 1.5 T MRI system.

To further validate our MM lens, an experiment was done to test the working frequency of the proposed device. We tested the signal responses at both sides of the MM lens with the help of a R&S®ZVB Vector Network Analyzer, whose frequency ranges from 10 MHz to 24GHz with four test ports. In the experiments demonstrated in Fig. 2(b), port 1 loaded with a magnetic dipole antenna was used as source and port 2 was used as the detector. The experiments are divided into two steps: we first test the magnetic field intensity received at port 2 with the MM lens, and then remove the MM lens and test again, while other configurations are the same. Figs. 2(c)–(d) show the increment (between with and without the MM lens) of the magnetic field intensity of the system detected by a magnetic dipole antenna at port 2 from 50 MHz to 100 MHz. Fig. 2(c) shows that there is a significant enhancement at the specific frequency of 63.42 MHz, which is up to 3.2 dB. Additionally, we found that there is a significant resonance at 56 MHz. In order to check the reasons for these peaks, we change the size of the magnetic dipole antenna at port 1. The corresponding increment of the magnetic field intensity is shown in Fig. 2(d), from which we also see a significant enhancement at the same specific frequency of 63.42 MHz, while the resonance phenomenon is shifted to 52 MHz. The results are similar if we change the size of the magnetic dipole antenna (the detector) at port 2. According to the superlens theory proposed by Pendry [1], for a negative permeability MM lens with a small thickness and $\mu_r = -1$, the transmission ratio for the TE polarization can be approximated as $T = \exp(-ik_z d) = \exp(+\sqrt{k_x^2 + k_y^2}d)$, where $\vec{k} = (k_x, k_y, k_z)$ is the wave number. Therefore, we have $T > 1$, i.e., the evanescent field can be enhanced. Thus we can conclude that the significant enhancement of the magnetic field intensity at 63.42 MHz is due to the resonance of the MM lens, while the resonance phenomenon at a lower frequency is

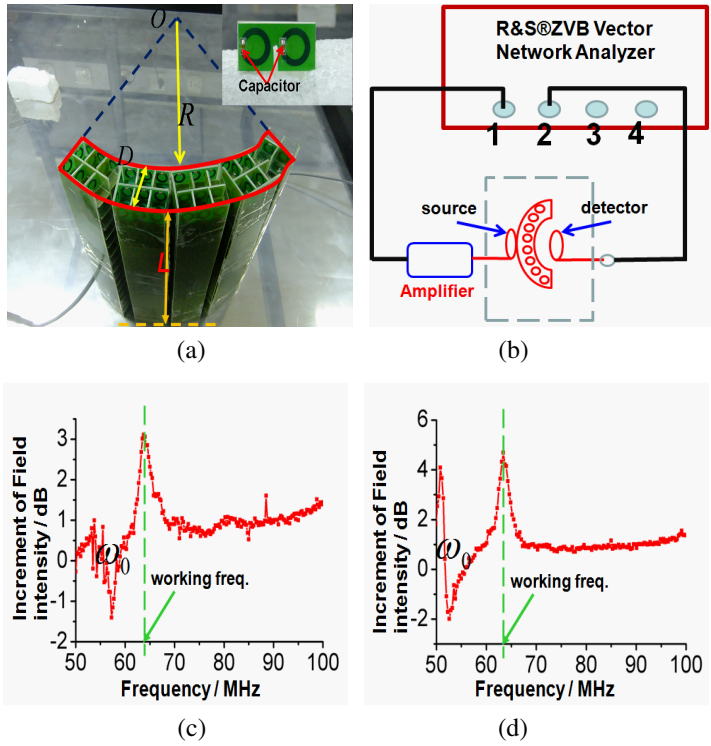

Figure 2. Signal responses are tested by R&S®ZVB vector network analyzers with and without the MM lens. (a) Photograph of the fabricated lens with R (10 cm) for the inner radius and D (3 cm) for thickness. The unit part consists of $16 \times 3 \times 2$ cubic cells and five unit parts are connected to each other. Each split-ring is loaded with a capacitor, as shown in the inset. (b) The experimental setups; (c) the increment of the magnetic field intensity measured with a specific magnetic dipole antenna at port 2; (d) the measured increment of the magnetic field intensity when changing the size of the magnetic dipole antenna at port 1, where ω_0 represents the intrinsic resonant frequency of the magnetic dipole antenna. Interestingly, for both cases there is a narrow-band response ofMM lens and a significant amplification at the frequency of 63.42 MHz.

due to the intrinsic resonance of the magnetic dipole antennas. The field enhancement occurs at 63.42 MHz for both cases, and this is consistent to the theoretical prediction of 63.58 MHz for the resonant frequency of the MM lens. The difference of the amplifications between

Fig. 2(c) (3.2 dB) and Fig. 2(c) (4.1 dB) is related to the emission efficiency of the magnetic dipole antenna. Our MM lens can be used in the practical 1.5 T MRI system.

The experiment was carried out in a General Electric (GE) Signa 1.5 T MRI system sited in the First Affiliated Hospital of College of Medicine, Zhejiang University (China). The standard 3 inch circular surface coil was used as the detector. Surface coils are usually used to obtain images of tissues in the proximity of the coil. The sensitivity of surface coils, as well as the SNR, decreases rapidly with the distance from the coil [13]. In the experiment, we have noticed that the coil may magnetically couple with the small unit cells that constitute the MM lens [5]. To avoid the situation, the loop of coil antenna has been retuned in the presence of our cylindrical rolled-up MM lens by the clinical researchers in the First Affiliated Hospital of College of Medicine, Zhejiang University (China). We used the standard water saline phantom with $12\times12\times18\,\mathrm{cm}^3$, which is filled with a hydroxyethyl cellulose solution doped with 1.5 g/l $CuSO_4$. Fig. 3 shows the MR images obtained for 3 inch surface coil, in the presence and in the absence of the MM lens. Both sagittal and coronal MR images are obtained. Fig. 3(a) and Fig. 3(b) show the experimental setups of 1.5 T MRI system both with and without MM lens, respectively. Fig. 3(a) shows the MM lens is closely placed between the coil and the phantom, while Fig. 3(b) shows that the coil is directly placed in contact with the phantom. By comparing the MR images in Fig. 3(c) and Fig. 3(d), it is apparent that the penetration depth has been increased in Fig. 3(c), in which the RF field is much stronger. On the other hand, Figs. 3(e), (f) shows the MR images at 2.5 cm in the water saline phantom. Comparing the signals of same locations at A and B, the image is more visible in Fig. 3(e) than that in Fig. 3(f). This means that the resolution of the surface coil has been improved due to the focusing property of our MM lens. This experiment clearly illustrates the ability of the cylindrical rolled-up MM lens to translate the field profiles of the coil deeper into the phantom and improve the sensitivity of surface coils. This means the rolled-up MM lens could be advantageously used in MRI techniques to obtain a better image of e.g. the brain or heart in the clinical research.

4. FURTHER WORK

Since the rolled-up MM lens suggested for MRI applications shows negative permeability, it is interesting to study the discrimination property of the fields coming from two independent sources due to its curvature. Fig. 4(a) sketches the configurations under analysis.

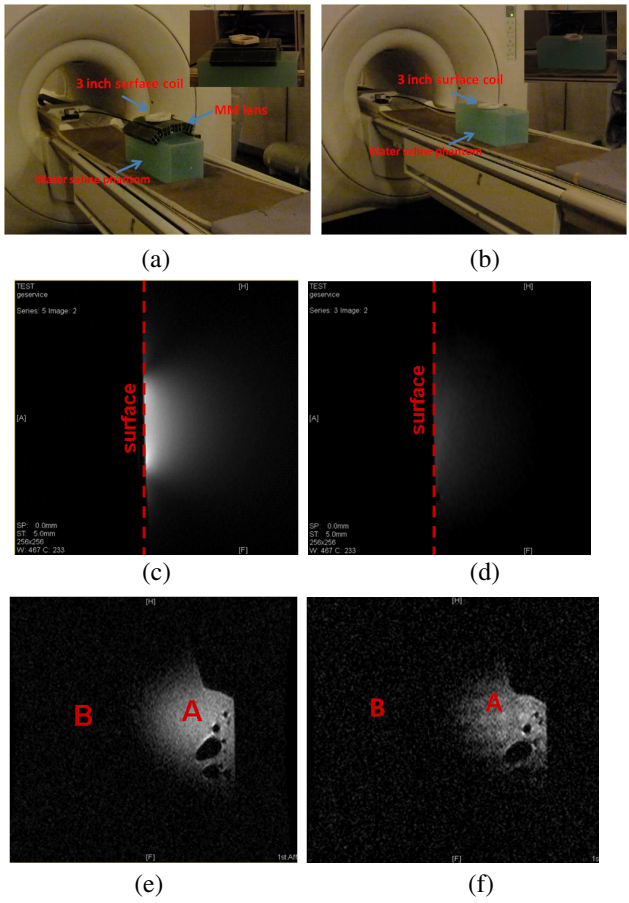

Figure 3. MR images are obtained for a standard 3 inch surface coil. The standard water saline phantom with a size of $12 \times 12 \times 18\,\mathrm{cm}^3$ is used. The red dashed line represents the surface of the phantom. (a), (b) Experimental setups with and without MM lens; (c), (e) when the MM lens is closely placed between the coil and the phantom; (d), (f) when the coil is placed in contact with the phantom. In particular, (c), (d) Sagittal images containing the axis of the coil; (e), (f) Coronal images at a distance of 2.5 cm inside the phantom. Comparing the images around location A and B, the image resolution has been improved by the MM lens.

Generally, two ideal point sources $(S1, S2)$ with normalized current density are placed within the circle of the lens. As is demonstrated above, the normal tissue is modeled as a cylinder inside the MM

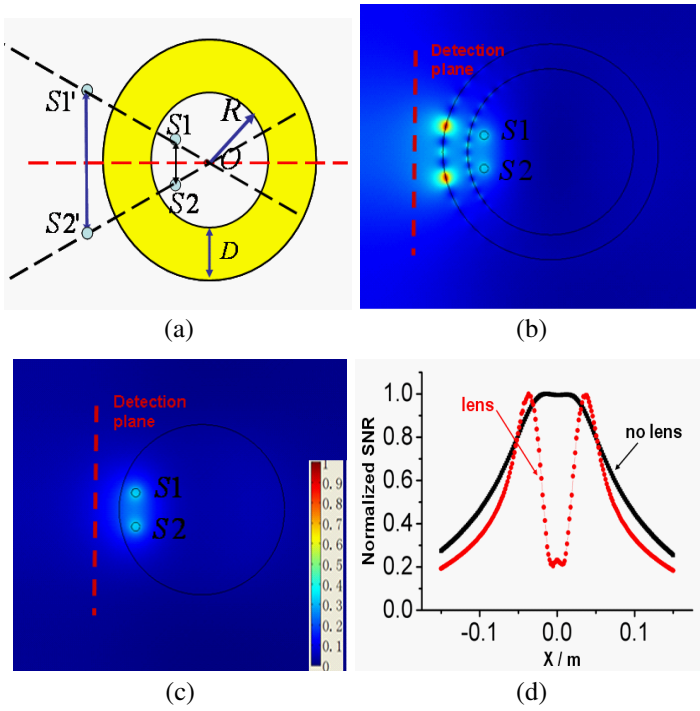

Figure 4. Magnetic field patterns of two independent sources. The rolled-up lens has R (10 cm) for the inner radius and D (3 cm) for thickness with $\mu_r = -1$. The two independent sources $(S1, S2)$ are 4 cm separated and 2 cm away from the surface of the lens. The permittivity of normal tissue inside the MM lesn is $\varepsilon \approx 21$, conductivity $\sigma = 0.11$, while the malignant tissues of $S1, S2$ is $\varepsilon \approx 80$, conductivity $\sigma = 0.77$. (a) Schematic diagram for the model; (b), (c) the normalized field distributions in the presence and in the absence of the lens, respectively; (d) the corresponding cross-sectional plot of normalized SNR at the selected detection plane.

lens. The permittivity is $\varepsilon \approx 21$, conductivity $\sigma = 0.11$, while the malignant tissue's permittivity is $\varepsilon \approx 80$, conductivity $\sigma = 0.77$. Fig. 4(b) and Fig. 4(c) shows the discrimination of magnetic field with and without the MM lens, respectively. The lens is set to 10 cm in the inner radius and 3 cm thick, while the two independent sources $(S1, S2)$ are 4 cm separated and 2 cm away from the surface of the lens. Our simulation results indicate that our cylindrical MM lens can transfer the two sources towards to the detection plane as if the separation between the two images are much wider (8 cm separated;

two times increase of the separation) than the actual separation of the two sources. Therefore, our cylindrical MM lens can give a better image resolution than a traditional slab MM lens [17]. With an appropriately design of the lens, the spatial resolution could be enhanced (much better than the traditional MM slab [4]). Furthermore, Fig. 4(d) clearly depicts how the rolled-up lens can improve the discrimination between the fields coming from two independent sources. We choose the same distance (3 cm away) for the detection plane from the surface of the cylindrical MM Lens (Fig. 4(b)) or the phantom (Fig. 4(c)). The SNR is significant stronger at the two central focusing spots, which can be clearly distinguished. Therefore, an improvement of the MRI imaging resolution is expected. Meanwhile, the operating frequency in a 1.5 T system is around 63.855 MHz, so that the wavelength corresponds to 5 meters. Fig. 4(d) shows that our rolled-up MM lens can give a near field imaging with a better resolution. And this is especially useful in brain [8] or breast imaging, for which high spatial resolution is required.

5. CONCLUSION AND DISCUSSION

In this paper, a rolled-up negative permeability lens for MRI has been proposed and numerical simulations have been performed with the finite element method (FEM) using commercial (COMSOL Multiphysics) software. Meanwhile, the experiment has been carried out with R&S®ZVB Vector Network Analyzer to validate the resonant working frequency of the fabricated MM lens. We have also done some clinical experiments to validate that the MM lenses have the ability to improve the sensitivity of the surface coil. To keep consistent with our numerical simulation results in the present paper, we fabricated a cylindrical MM lens with an inner radius of 10 cm and a thickness of 3 cm. The rolled-up lens is flexible and can be in close contact with the body of a patient. The design of the rolled-up MM lens consisting of capacitive-loaded copper split-rings can be further improved to satisfy the practical 1.5 T or 3 T MRI systems. The MM lens could provide a way to increase spatial resolution while still fulfilling the safety regulations on the field strength of the coils. In general, we believe that our rolled-up MM lens could help to improve several aspects of MRI performance, such as the penetration depth and spatial resolution.

ACKNOWLEDGMENT

The authors are grateful to Dr. Qidong Wang of the First Affiliated Hospital of College of Medicine, Zhejiang University (China) for his help in clinical experiment, and Dr. Yungui Ma and Yi Jin for

helpful discussion. The partial support of the National Natural Science Foundation of China (NSFC) (under Grants 60990322 and 61178062) is gratefully acknowledged.

REFERENCES

1. Pendry, J. B., "Negative refraction makes a perfect lens," *Physical Review Letter*, Vol. 85, 3966, 2000.
2. Hornak, J. P., "The Basics of MRI," URL, http://www.cis.rit.edu/htbooks/mri/index.html, 1996.
3. Freire, M. J., L. Jelinek, R. Marques, and M. Lapine, "On the applications of $\mu = -1$ metamaterial lenses for magnetic resonance imaging," *Journal of Magnetic Resonance*, Vol. 203, 81, 2010.
4. Freire, M. J., R. Marques, and L. Jelinek, "Experimental demonstration of a $\mu = -1$ metamaterial lens for magnetic resonance imaging," *Applied Physics Letter*, Vol. 93, 231108, 2008.
5. Lopez, M. A., et al., "Nonlinear split-ring metamaterial slabs for magnetic resonance imaging," *Applied Physics Letter*, Vol. 98, 133508, 2011.
6. Wiltshire, M. C. K., J. B. Pendry, I. R. Young, D. J. Larkman, D. J. Gilderdale, and J. V. Hajnal, "Microstructured magnetic materials for RF flux guides in magnetic resonance imaging," *Science*, Vol. 291, No. 5505, 2001.
7. Radu, X., D. Garray, and C. Craeye, "Toward a wire medium endoscope for MRI imaging," *Metamaterials*, Vol. 3, No. 2, 90–99, 2009.
8. Wiggins, G. C., J. R. Polimeni, A. Potthast, M. Schmitt, V. Alagappan, and L. L. Wald, "96-channel receive-only head coil for 3 Tesla: design optimization and evaluation," *Magnetic Resonance in Medicine*, Vol. 62, No. 3, 754–762, 2009.
9. Fear, E. C., X. Li, S. C. Hagness, and M. A. Stuchly, "Confocal microwave imaging for breast cancer detection: Localization of tumors in three dimensions," *IEEE Transactions on Biomedical Engineering*, Vol. 49, No. 8, 2002.
10. Mohsin, S. A., N. M. Sheikh, and U. Saeed, "MRI induced heating of deep brain stimulation leads: Effect of the air-tissue interface," *Progress In Electromagnetics Research*, Vol. 83, 81–91, 2008.
11. Insko, E. K., M. A. Elliott, J. C. Schotland, and J. S. Leigh, "Generalized reciprocity," *Journal of Magnetic Resonance*, Vol. 131, 111, 1998.
12. Baena, J. D., L. Jelinek, R. Marqués, and M. Silveirinha, "Unified

homogenization theory for magnetoinductive and electromagnetic waves in split-ring metamaterials," *Physical Review A*, Vol. 78, 013842, 2008.

13. Rennings, A., P. Schneider, S. Otto, D. Erni, C. Caloz, and M. E. Ladd, "A CRLH zeroth-order resonant antenna (ZORA) with high near-field polarization purity used as an RF coil element for ultra high field MRI," *Metamaterials*, 13–16, 2010.
14. Gong, Y. and G. Wang, "Superficial tumor hyperthermia with flat left-handed metamaterial lens," *Progress In Electromagnetics Research*, Vol. 98, 389–405, 2009.
15. Lapine, M., L. Jelinek, M. J. Freire, and R. Marqués, "Realistic metamaterial lenses: Limitations imposed by discrete structure," *Physical Review B*, Vol. 82, 165124, 2010.
16. Sydoruk, O., E. Tatartschuk, E. Shamonina, and L. Solymar, "Resonant frequency of singly split single ring resonators: An analytical and numerical study," *Metamaterials*, 632–634, 2008.
17. Algarin, J. M., M. J. Freire, M. A. Lopez, M. Lapine, P. M. Jakob, V. C. Behr, and R. Marqués, "Analysis of the resolution of split-ring metamaterial lenses with application in parallel magnetic resonance imaging," *Applied Physics Letter,* Vol. 98, 014105, 2011.
18. Joines, W. T., Y. Zhang, C. Li, and R. L. Jirtle, "The measured electrical properties of normal and malignant human tissues from 50 to 900 MHz," *Medical Physics*, Vol. 21, 547, 1994.